Dynamics of the fragmentation of D_2 by fast protons and slow highly charged Xe^{26+}

I. Ali,[1] R. D. DuBois,[2] C. L. Cocke,[1,*] S. Hagmann,[1] C. R. Feeler,[2] and R. E. Olson[2]
[1]*Department of Physics, Kansas State University, Manhattan, Kansas 66506*
[2]*Department of Physics, University of Missouri-Rolla, Rolla, Missouri 65409*
(Received 23 February 2001; published 12 July 2001)

Using recoil-ion momentum spectroscopy, combined with a multihit detector system, the full momentum vectors of both fragment ions produced by fragmentation of D_2 by fast 50-kV protons and slow (9.56–0.191 keV/u) Xe^{26+} ions have been measured. The data are kinematically complete, and make it possible to separate the laboratory momentum of the center of mass of the molecule from the momentum of each fragment in the center-of-mass system of the molecule. Using this separation, we find that, for higher collision velocities, the overall reaction can be described as double-electron capture, followed in a second and separate step by a Coulomb explosion of the doubly charged D_2 molecule. For the lowest collision velocities, however, the projectile remains in the vicinity of the molecule during the fragmentation, and this clean separation of steps is lost. The projectile is found to extract internal energy from the molecule, thus leading to less energetic fragments in the center-of-mass system of the molecule. This effect causes a distortion in the spherical momentum images, as shown by the two-dimensional momentum distributions in the collision plane. The experimental results are found to be in good agreement with five-body classical trajectory Monte Carlo calculations.

DOI: 10.1103/PhysRevA.64.022712 PACS number(s): 34.50.Fa, 39.30.+w

I. INTRODUCTION

While the static properties of many-particle atomic and molecular systems are often understood in great detail, largely through electron and photon spectroscopy, the same cannot be said of dynamic processes involving such systems. This situation is partially due to the fact that a theoretical treatment of many-body dynamics is extremely complex. It is also due to the lack of experimental data which provide comprehensive coverage of the correlated momenta of reaction products in many-body final states. Over the years, a number of experimental studies of collisionally induced molecular fragmentation has been carried out using coincidence techniques to examine correlations between momenta of the fragments (for example, see Refs. [1–6]). When dispersive spectrometers are used for an energy analysis of the fragments, the experiments have usually been sufficiently time-consuming that full coverage of the final momentum space was not feasible. Significant advances in this respect have been made in recent years through the use of imaging detectors [7–10] to record, in multiple coincidence, the correlated momenta of all reaction products [11–13]. This approach has made possible kinematically complete experiments in which comprehensive coverage of the entire multiple-dimensional final momentum space is achieved.

In this paper we address the many-particle nature of the collision-induced breakup of a molecule for a situation in which the projectile is present during both the excitation and dissociation stages of the process. We report on an experimental study of the breakup of the diatomic molecule D_2 induced by a collision of this molecule with slow, highly charged xenon ions. This process involves two nuclei and two electrons, plus the projectile ion. Because of the huge mass difference, the electrons react to the perturbing potential of the projectile much faster than the nuclei. If the molecular dissociation is induced by fast ion or electron impact, the standard picture for molecular dissociation is that it is a two-step process: a fast Frank-Condon electronic transition to a dissociating molecular state is followed, in a second step, by slow Coulomb explosion of the heavy nuclei. In the case studied here, double electron capture by a slow Xe^{26+} ion, the initial process is an overbarrier capture which proceeds with high efficiency even at extremely slow projectile velocities. In this case the interaction time is long, due to the low collision velocity and the large interaction distance. When the interaction time becomes comparable to the fragmentation time, the projectile field will strongly influence the fragmentation dynamics. In this case, the two-step picture fails and the dissociation dynamics are controlled by Coulomb interactions among all the heavy particles.

In accordance with these expectations, recent theoretical studies employing the classical trajectory Monte Carlo (CTMC) method predicted strong three-body effects between the molecular fragments and the projectile ion as the collision velocity was decreased for dissociation of D_2 by various ions [14,15]. These predictions were consistent with several experimental observations [16–20]. Most of these experimental studies only measured the momentum of one fragment in the laboratory frame. Thus it was difficult to interpret the data unambiguously. In the present experiment we have carried out a kinematically complete measurement of the process. The momenta of both of dissociation fragments are measured, allowing us to separate the momentum transferred to the molecule as a whole in the capture process from that released to the fragments in the dissociation. In an earlier paper [21], we reported preliminary results of this experiment. This paper presents a much more complete data set and interpretation, as well as results from an analysis of the momentum distribution with experimentally determined collision plane.

*Corresponding author. FAX:+785-532-6806. Email address: cocke@phys.ksu.edu

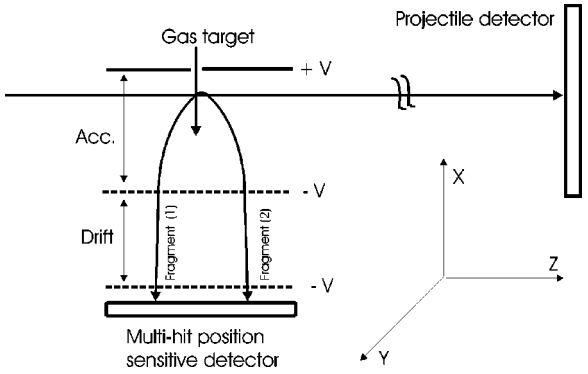

FIG. 1. Experimental setup.

II. EXPERIMENTAL SETUP

This experiment was performed using the EBIS facility of the JRM Laboratory at Kansas State University. The experimental arrangement is shown in Fig. 1. The Xe^{26+} beam was collimated to a beam spot of less than 1 mm^2 by two pairs of collimators. The beam intersected a D_2 beam effusing from a microchannel array. The density was approximately (10^{14} molecule/cm^3). The molecular ionic fragments were extracted by an electrostatic field (60 V/cm), before they entered a field-free region followed by a position-sensitive detector. The charge-changed projectile was detected 1 m downstream by a second position-sensitive detector. The position sensitivity of this detector was used to identify projectile charge states only. Both D^+ ions from the dissociation of D_2 were detected in coincidence with the projectile, using a position-sensitive multihit detector. This detector is based on a fast-timing delay-line position and time readout, as explained in a previous work [7]. For each fragment, the time of flight and position on the detector were measured, and all three components of the momentum vector were calculated. The accuracy of these components was determined in part by uncertainties in the time measurement (typically less than 2 ns, electronic contribution), the position resolution of the delay-line detectors (0.5 mm), and the interaction dimensions.

Because relatively energetic fragments are produced in this experiment, a high extraction field was used to collect fragments emitted in all directions. It was found that a field of 60 V/cm was enough to collect D^+ ions with high kinetic energies ($\leqslant 60$ eV) emitted in all directions with a high efficiency. Fragments arriving at the detector sequentially in time were processed if they were separated by at least 10 ns. This leads to a ''dead time window,'' as can be seen in the data. However, the arrival time difference depends on the energies, directions, and extraction field. For the field used in this experiment, the time difference was 0–300 ns. Thus loss of particle pairs due to double-pulse resolution was less than 10%.

There are different factors that limited the momentum resolution in this experiment. The major contributor in the z direction was the 3-mm length of the interaction region along the beam. This resulted in an uncertainty in momentum of approximately 4 a.u. (due mainly to the uncertainty in the relative positions of collision and hit, not of the flight time of the recoil ion). The thermal motion contributed approximately 4-a.u. uncertainty to the y momentum. The uncertainty in the x momentum is caused by errors in timing on the projectile, which can be as large as 15 ns (slowest beam). For a 60-V/cm extraction field, this leads to an x-momentum uncertainty of 7 a.u. The timing errors come from the finite extent of the target as well as from beam energy uncertainties. The measured momentum resolution of the system was found to be approximately ± 5 a.u., consistent with the above estimates. Much of this uncertainty disappears when the momenta in the center of mass of the molecule are calculated.

The momentum vectors for both fragments, $\mathbf{k}_1$ and $\mathbf{k}_2$, were calculated in the laboratory frame on an event-by-event basis. Referring to the coordinate system shown in Fig. 1, the y and z components were determined from the impact position on the detector. The x component was calculated from the flight time of the fragment, using the projectile impact as the time reference.

Using the two-step model as a starting point, one can think of the final momenum of each fragment as originating from two contributions: (a) the momentum transferred from the projectile to the center of mass of the molecule during the capture process, and (b) the momentum gained through the Coulomb repulsion between the fragment ions during the dissociation stage. These momentum contributions can be separated by calculating, on an event-by-event basis, the Jacobi momenta. In this paper we define these to be $\mathbf{k}=(\mathbf{k}_1-\mathbf{k}_2)/2$ and $\mathbf{K}=(\mathbf{k}_1+\mathbf{k}_2)/2$. (This definition is adopted in order that the laboratory momenta be simply the sum and difference of $\mathbf{K}$ and $\mathbf{k}$; this somewhat facilitates a comparison of the laboratory and Jacobi-coordinate spectra presented here). In terms of these coordinates, the momentum transferred from the projectile to the center of mass is given by two times $\mathbf{K}$, and the momentum gained by each ion from the Coulomb repulsion of the ions in the center of mass is given by $\mathbf{k}$. Also note that any effects due to extension of the molecular gas target are eliminated in the $\mathbf{k}$ spectra, since the position for each collision is determined from the positions of the detected fragments.

III. RESULTS AND DISCUSSION

A. Laboratory momentum spectra

Figure 2 shows two-dimensional momentum distributions for one fragment in the laboratory frame $\mathbf{k}_1$ or $\mathbf{k}_2$. These spectra show momentum slices in the x-y plane of the Coulomb explosion spheres, formed by requiring that the momentum in the z direction be less than 10 a.u. Thus they represent transverse momentum slices for an observer looking along the beam axis. The gap in the data near $k_{1x}=0$ is instrumental in nature, and is due to the finite pulse-pair resolution. Five systems are shown, ordered from top to bottom according to increasing perturbation, q/v, by the projectile. Here q and v are the projectile charge and velocity in a.u.; (a) is for the least perturbing projectile studied, 50-keV protons ($q/v=0.71$ a.u.). (b)–(e) are for ever-decreasing energy, i.e., increasing perturbation strength, Xe^{26+} impact: (b) for 9.56 keV/u, $q/v=42$; (c) for 764 eV/u, $q/v=149$;

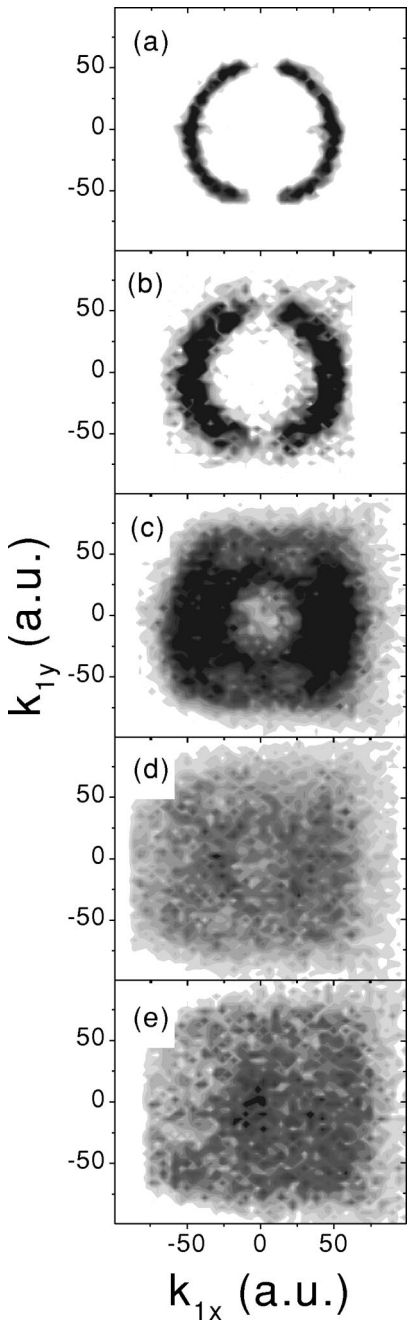

FIG. 2. Two-dimensional distributions of the transverse momentum in the laboratory frame k_{y1} vs k_{x1} for the dissociation of D_2 by (a) 50-keV protons; (b)–(e) are for a decreasing energy Xe^{26+}, with (b) 9.56 keV/u, (c) 764 eV/u, (d) 382 eV/u, and (e) 191 eV/u.

(d) for 382 eV/u, $q/v=211$; and (e) for the most highly perturbing case studied, 191 eV/u, $q/v=298$. Observe that as q/v increases, the transverse spectra show an evolution from a narrow Coulomb explosion ring of radius near 50 a.u. in momentum to a highly diffuse distribution having a broad range of momenta extending from zero to nearly 100 a.u. A radius of 51 a.u. is expected from two deuterons exploding from a resting, doubly charged D_2 molecule, beginning at the equilibrium internuclear separation of the neutral D_2 molecule.

As demonstrated in recent works [21,19], the change of the laboratory-frame momentum spectrum from a well-defined Coulomb sphere to a highly diffuse momentum distribution can result from the vector addition of the momentum gained by the Coulomb repulsion between the charged molecular fragments and the momentum transferred from the projectile to the center of mass of the molecule. As discussed below, in this experiment we separate these two contributions experimentally. If only the laboratory momentum of single fragments is measured, the latter momentum contribution can be calculated from a model description of the capture process [19].

B. Momentum transfer to the molecular system: K spectra

The next two figures show spectra of the collisional momentum transfer to the molecule, **K**. The left-hand column of each figure shows two-dimensional projections. Figure 3 shows **K** momenta projected into the x-y (i.e., transverse) plane, while Fig. 4 shows **K** momentum slices projected into the x-z plane. On the right side of Fig. 3 is shown a slice through the x-y spectrum, formed by requiring that K_y be less than $+/-$ 10 a.u.; on the right side of Fig. 4 is shown a projection of the x-z spectrum onto the z axis (i.e., the longitudinal momentum profile). The collision systems are the same as in Fig. 2.

For fast proton impact, the transverse momentum transfer to the center of mass of the dissociating molecule is small. Thus, in this case, the laboratory momenta of the fragments result mainly from the Coulomb explosion of the molecule. The proton data also provide information about the momentum resolution which can be used to evaluate the xenon impact data. For increasing perturbation strength, ever-increasing amounts of transverse momentum are transferred from the projectile to the center of mass of the molecule. This is illustrated by the right side of the figure. The maximum of the momentum distributions in the right column of Fig. 3 move to higher values of K_x in a linear fashion when plotted versus the reciprocal of the collision velocity. At the extreme of the systems studied, nearly 50 a.u. of momentum are transferred. This is comparable to the momentum gained by each D^+ ion from the Coulomb repulsion after the electrons are removed from the molecule.

These spectra are consistent with previous measurements of momentum-transfer distributions and Q value measurements for capture from neutral monotonic targets by slow, highly charged projectiles. [Here Q is the the binding energy of the electron(s) after capture minus that before.] This process has been heavily studied over the past two decades [22–24], and is rather well understood. For example, the donut-shaped features of the transversal momentum distributions and increasing radius with decreasing collision velocity were previously noted in numerous works involving capture and ionization of atoms (e.g., Refs. [25,26]) in collisions with slow, highly charged ions. The backwards shifts seen in the longitidunal momentum spectra are due to the positive Q value of the capture reaction, which throws the projectile forward and the recoil ion backward (e.g., see Ref. [26]).

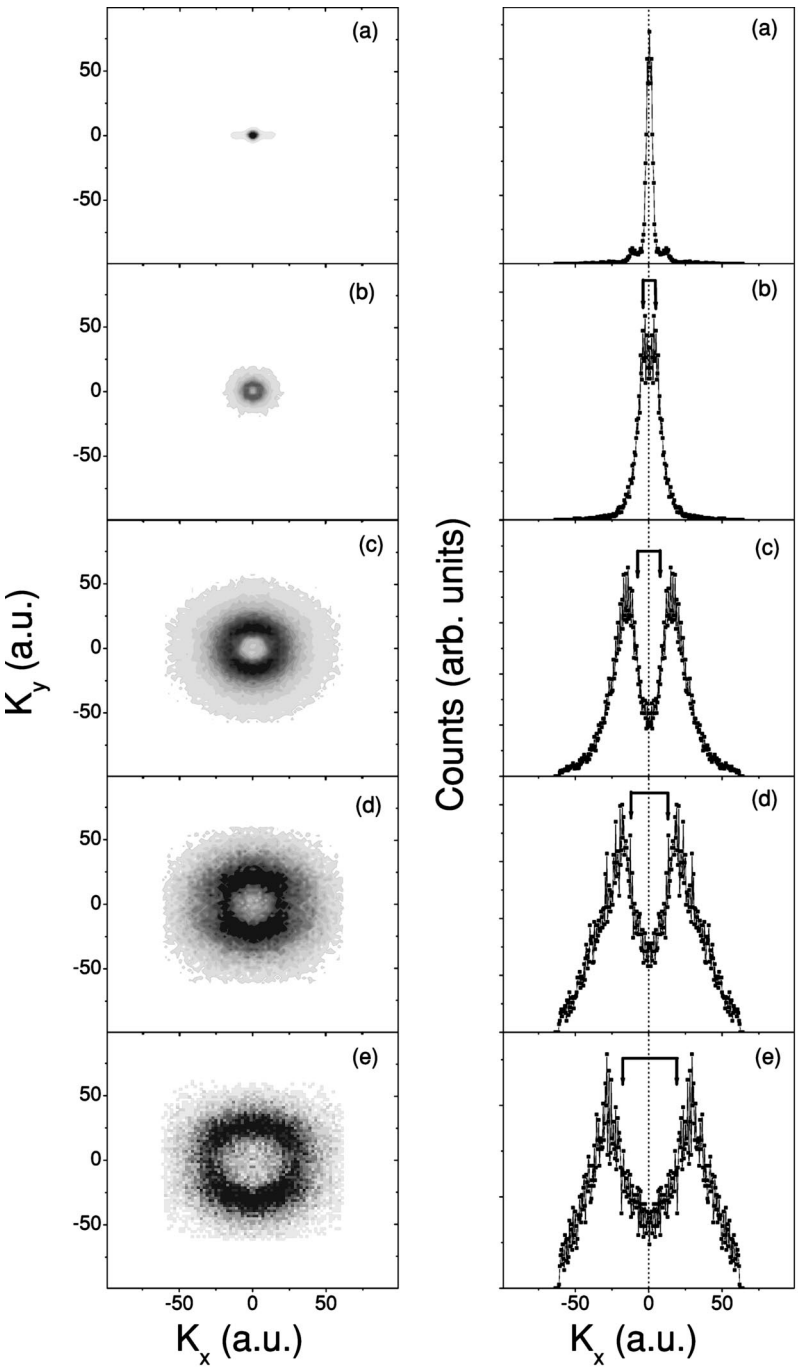

FIG. 3. The left column represents two-dimensional momentum distributions of K_y vs K_x (transverse to the beam). The collision systems are the same as in Fig. 2. The right column represents the corresponding one-dimensional distributions (K_y) of the momentum transferred from the projectile to the center of mass of the dissociating molecule (D_2) for projectiles indicated in the left column. The one dimensional distributions are produced by taking the projection of ± 10 a.u. momentum slices about the origin of the two-dimensional distributions.

We have used the extended over-barrier model of Niehaus [24] to calculate expected longitudinal shifts for this case. We have assumed a two-electron target with binding energies of 15.5 and 35 eV, the first and second ionization energies of the D_2 molecule for fixed internuclear distance. The results show that the capture of the second electron occurs at an internuclear distance of 13 a.u., and results in an energy gain of 3.1 a.u. From these values, one can calculate the expected longitudinal momentum transfer to the recoil ion, using the equation

$$p_{\|} = -\frac{Q}{v} + \frac{iv}{2}, \tag{1}$$

where v is the beam velocity, i is the number of electrons transferred (two here), and atomic units are used. The resulting calculated values are shown by arrows in the right-hand column of Fig. 4. These values are consistent with, if somewhat smaller than, the observed shifts. Indeed, it is clear that the longitudinal momentum spectra are more complex than this model can describe, since even structure is seen at the lowest velocity. These spectra can be compared directly to recoil-momentum-spectroscopy spectra measured by Abdallah *et al.* [25]. In that study, it was established that the double capture Q-value spectra have considerable structure. The values of Q measured were slightly larger than those predicted by the Niehaus model. Thus we believe that the

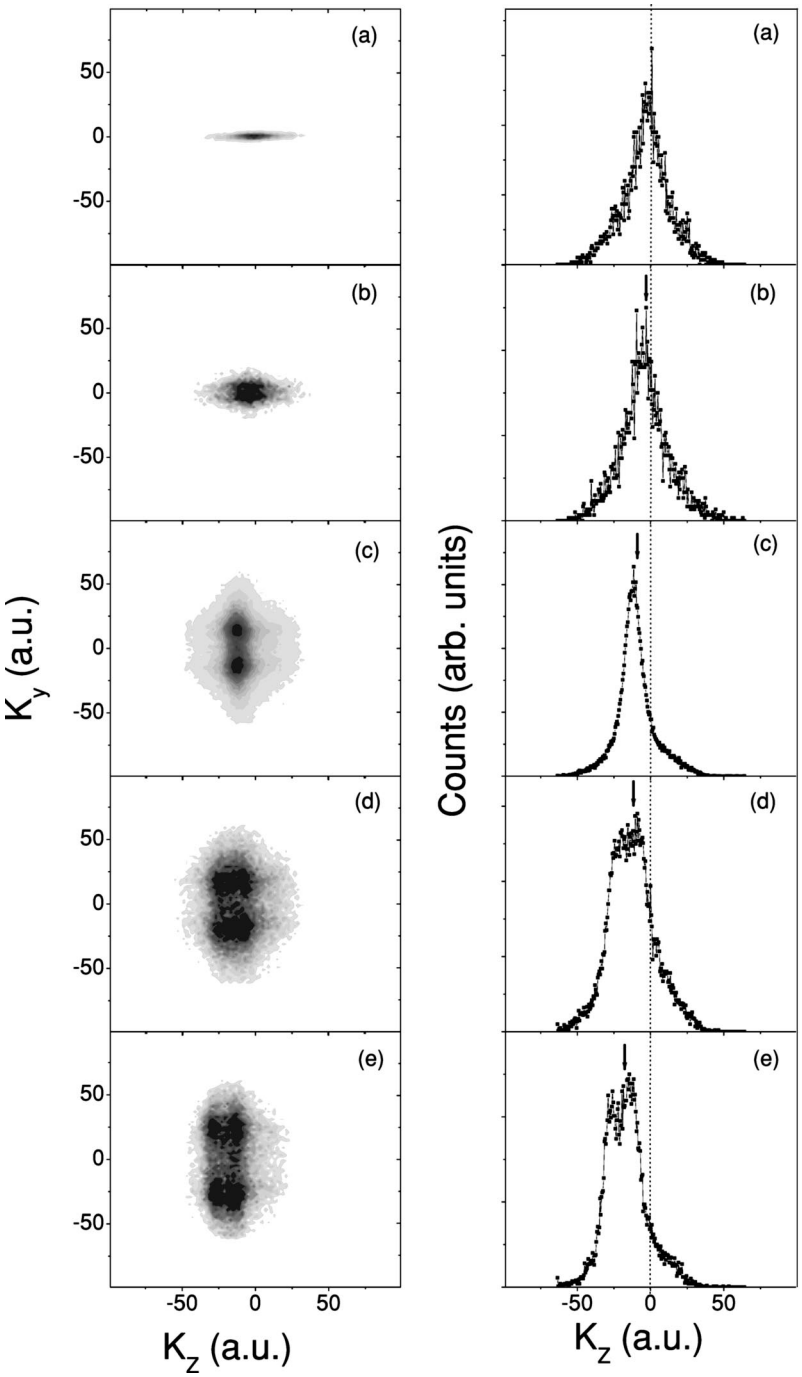

FIG. 4. The left column represents two-dimensional momentum distributions of K_y (transverse to the beam) vs K_z (parallel to the beam). The collision systems are the same as in Fig. 2. The right column represents the corresponding one-dimensional distributions of the longitudinal momentum transferred from the projectile to the center of mass of the dissociating molecule (D_2).

present longitudinal *K* spectra are consistent with expectations for the two electron transfer process.

One can also calculate the transverse momentum transfers expected for the Niehaus model, but we prefer here the simpler approach of calculating the momentum transfer which would occur were the capture to occur at a single localized crossing between the initial channel $(Xe^{26+}+D_2)$ and the final one $(Xe^{24+}+D_2{}^{2+}$, where the Xe ion is in a state of excitation corresponding to a *Q* value of 3.1 a.u.). From studies such as that of Abdallah *et al.* [25], it is known that this slightly underestimates the transverse momentum transfer, but reproduces well the dependence on *Q* value, beam velocity, and so forth. This simple analysis, which is equivalent to taking the well-known half-Coulomb angle for projectile scattering, leads to the simple equation

$$p_{\perp} = -\frac{Q}{v}. \tag{2}$$

The results from evaluating this equation are shown as arrows in Fig. 3, where it is seen that the slight systematic underestimation of the transverse momentum transfer is again seen. The present observations for the transverse **K** spectra are thus also consistent with the existing understanding of the two-electron transfer process.

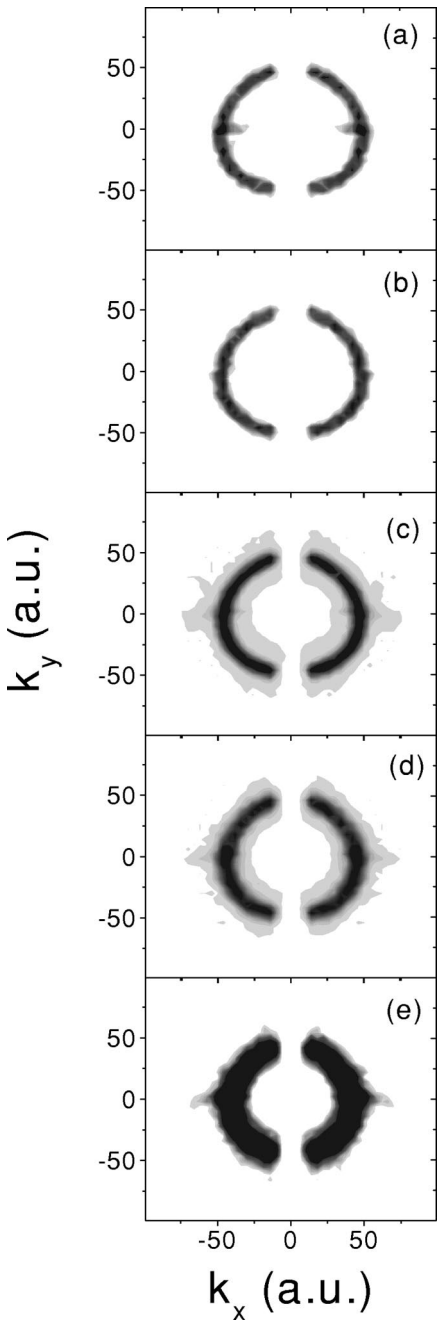

FIG. 5. Two-dimensional momentum distributions of k_y vs k_x (transverse to the beam). The collision systems are the same as in Fig. 2. The momentum distributions are produced by taking slices of ± 10-a.u. momentum about the origin of the momentum sphere.

C. Momentum of the fragments in the center-of-mass frame: k spectra

Figure 5 shows two-dimensional momentum distributions of the momentum of one fragment in the center of mass calculated using the Jacobi coordinate **k**. These momentum distributions are formed by cutting slices in the transverse plane (x-y plane) through the center of the Coulomb explosion spheres with a width of 20 a.u. Figure 6 shows the internal kinetic energy of one fragment in the center of mass

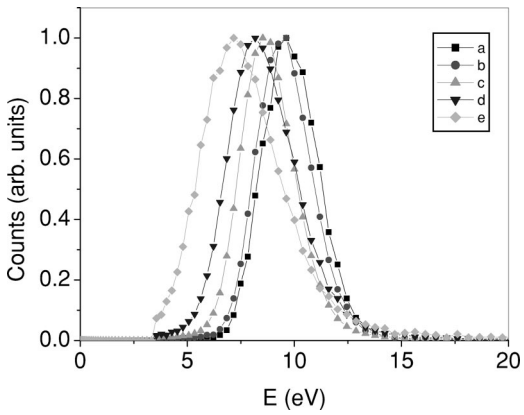

FIG. 6. Internal kinetic energy for D^+ fragments in the center-of-mass coordinate system of the molecule. Collision systems (a)–(e) are the same as in Fig. 2. All spectra are normalized to unity at their maxima.

of the dissociating molecule. The vertical scales of the energy distributions have been normalized to unity for display purposes. The collision systems are the same as in Fig. 2.

The **k** momentum distributions provide information about the internal energy in the center of mass of the D_2^{2+} molecule and the interaction of the molecular ions with the time-dependent strong electric field of the slow highly charged projectile. In the case of the dissociation of the molecule with protons and high energy (down to 2 keV/u) Xe^{26+}, the internal kinetic energy results merely from the Coulomb interaction of the positive deuterons with an energy of about 9.7 eV. This behavior indicates that the broadening of the momentum distributions in the laboratory frame results mainly from the vector addition of the momentum transferred to the center of mass of the molecule, plus the internal momentum of the fragments in the center of mass gained by the Coulomb interaction of the molecular ions. This vector addition of the momenta is in accordance with the predictions of the CTMC calculations [15], and supports the picture of the dissociation process as a two-step process [19–21].

In the case of the dissociation of the molecule with low impact energy Xe^{26+}, the **k** spectra show a systematic shrink in the spherical shell of the momentum distribution. This behavior is represented more clearly in the internal energy distributions (Fig. 6), which show a shift towards lower-energy values as well as an increase in the width of the distribution as the velocity of the projectile decreases. This effect represents a true three-body effect resulting from the interaction of the positive deuterons individually with the projectile. In order to understand this effect, we have to consider high-order components of the interaction between the projectile electric field and the D_2^{2+} system. For the dissociation of the molecule with a high-velocity projectile leading to a two-step dissociation, the dominant interaction with the projectile results from a dipole component that acts equally on both D^+ ions, leading to a transmission of momentum to the whole molecule. In collision with very slow Xe^{26+}, the projectile spends sufficient time in the vicinity of the dissociating molecule that the deuterons have enough

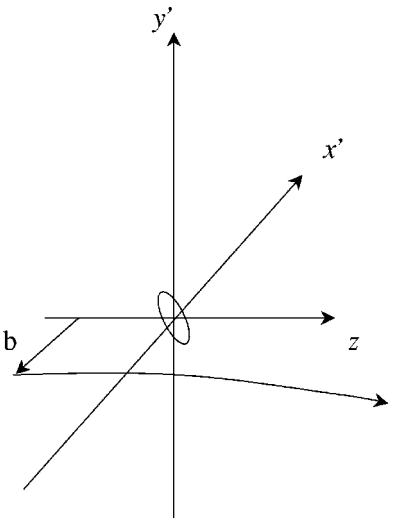

FIG. 7. Coordinate system used to show k spectra with fixed collision plane. The vector **K** is made to lie in the x'-z plane, pointing in toward positive x'. The path of the projectile thus lies in the x'-z plane, with impact parameter **b** as shown.

time to separate in space and interact with the projectile individually. In this case, quadrupole and higher-order components of the projectile field come into play. (We refer to a multipole expansion taken about the target origin.) For example, a quadrupole field will act differently on the two fragments, depending on the location of each fragment. The one closer to the projectile will be repelled more than the fragment farther away. As we have seen above, the capture process takes place at an impact parameter (16 a.u.) much larger than the initial inter-nuclear distance of the molecule (1.4 a.u.). When the projectile is outside the extent of the exploding molecule, the effect of the quadrupole part of the projectile field will be to remove internal energy from the ion pair, as seen in Fig. 6.

D. k spectra for experimentally determined collision plane

Because **K** is measured for each event, it is possible use the transverse **K** vector to determine the collision plane for each event. That is, we perform an event-by-event rotation about the z axis from the (x,y) laboratory frame to an (x',y') frame such that the transverse component of the vector **K**, lies along the positive x' axis (see Fig. 7). We note that the momentum transfer to the projectile is the negative of **K**, and thus the impact parameter **b** lies along the negative x' axis. In Fig. 8 we show **k** spectra in the primed system. In this system, $k_{x'}$ and $k_{y'}$, respectively, are the components of **k** lying in and perpendicular to the collision plane defined by the transverse component of **K**. The four rows in Fig. 8 correspond to Xe^{26+} energies of 9.56 keV/u, 764 eV/u, and 191 eV/u, proceding to slower projectiles as one moves downward in the figure. Each figure corresponds to a slice in the (now distorted) **k** Coulomb-explosion sphere, formed by requiring that the magnitude of the momentum vector not plotted be less than 10 a.u. In the left-hand column, the projectile can be visualized as passing from left to right along a straight line located in the plane of the page and below the molecule; in the center column, it passes from left to right but along a line located above the page and on the y' axis; in the right-hand column, it passes out of the page through a point somewhere on the $k_{y'}=0$ axis, and to the left of the molecule. Figure 8 shows that the Coulomb explosion sphere is distorted, most markedly for the slowest collision system (bottom row). We attribute this to the following physical process. The charge-transfer process does not begin until the projectile passes within about 16 a.u. of the target molecule; the major contribution to the cross section comes for impact parameters near this distance. Thus the Coulomb explosion should begin with the projectile located approximately at $x'=-16$ a.u. and $y'=0$. As the explosion proceeds, those molecules which are exploding along a line directed toward the departing projectile will have their internal energies most strongly perturbed by the projectile Coulomb field. Deuterons ejected toward the projectile will be preferentially slowed, while their partners ejected away will not be correspondingly accelerated as much because they are farther away. Thus the Coulomb sphere will be flattened along a direction facing the average location of the exiting projecile during the fragmentation process. This will be most easily seen when looking down on the collision plane from above (lower-left-hand figure), where the projectile acting on the exploding molecule is located in the (negative x', positive z) quadrant. The flattening is also observable, but less marked, when the Coulomb sphere is sliced along the other two views looking perpendicular to the collision plane.

These results are compared to corresponding theoretical CTMC calculations. For the calculation of a highly charged ion interacting with D_2, it is necessary to employ a five-body method that encompasses three nuclei and two electrons. Such a classical trajectory Monte Carlo model was described in detail by Wood and Olson [27] and Feeler *et al.* [15]. Concisely, Hamilton's equations of motion (30 coupled first-order differential equations) are iteratively solved for thousands of individual collisions in order to obtain sufficient statistics to study double-electron removal reactions. For an accurate description of the collision dynamics, it is important that the initial state represent the molecular environment along with its time evolution to the final products. Initially, the two electrons are bound to their parent nuclei by 13.6 eV. The individual deuterium atoms are bound to each other by a Morse potential whose equilibrium separation, dissociation energy and well curvature are determined by spectroscopic data [28]. The D_2 molecule is randomly oriented, with inter-nuclear separations appropriately weighted for the vibrational ground state in order to reproduce the distribution of deuteron kinetic energies produced in a vertical Franck-Condon transition. For an appropriate range of impact parameters, the passage of the highly charged ion is evolved in time. Throughout the collision process, all Coulomb interactions are included between the projectile and the four-body target, and between each electron and its parent nucleus. In our five-body calculations, the projectile's core electrons are ignored. This is justified since the reaction range is greater than an order-of-magnitude larger than the radial expectation values of the electrons. We dynamically model the molecular interactions intermediate to the $D^+ + D^+$ dissociated prod-

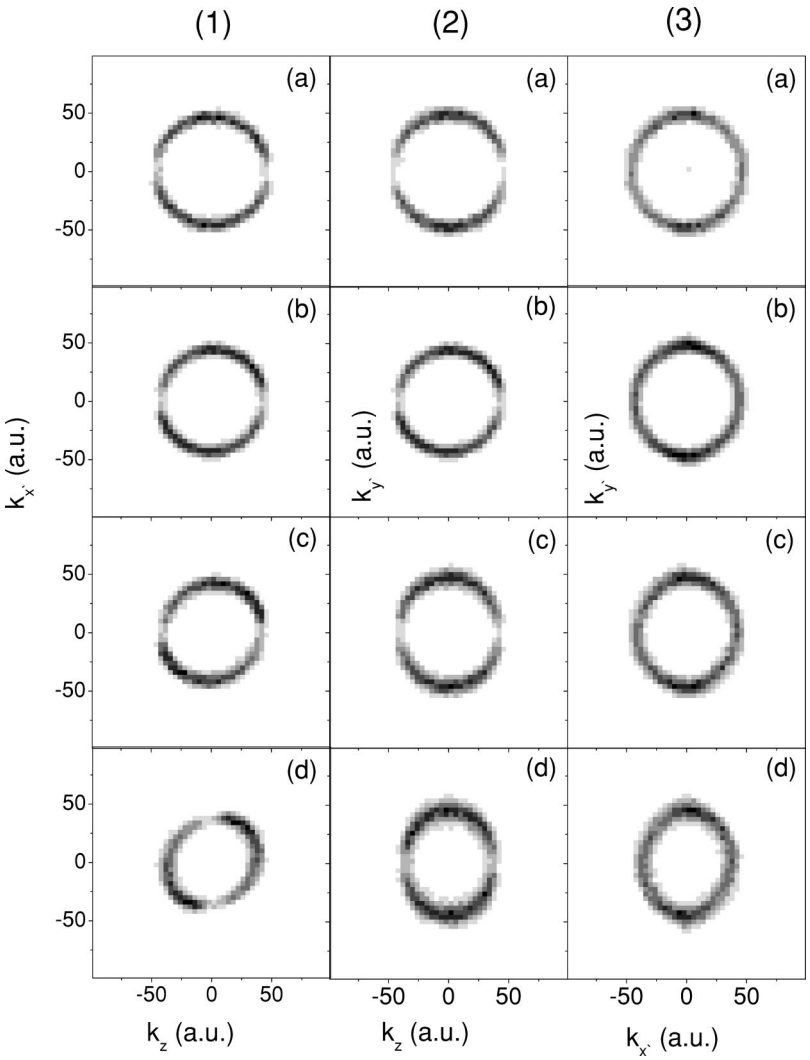

FIG. 8. The first column (1) represents the two-dimensional momentum distributions of $k_{x'}$ vs k_z. The collision systems, proceeding from top to bottom, are for Xe^{26+} energies of 9.56 keV/u, 764 eV/u, 382 eV/u, and 191 eV/u. The momentum distributions are produced by taking the slices of ± 10-a.u. momentum about the origin of the momentum sphere. The second and third columns (2) and (3) represent the slices in the other planes perpendicular to the collision plane. The gaps appearing in some of the rings are instrumental.

ucts. If one electron attains a positive energy relative to its parent nucleus during the collision, thus placing the molecule in the D_2^+ state, the electron-electron interaction is included in the Hamiltonian along with the Coulomb interactions between both electrons and the other target nuclear center. If the electron remaining on the molecule is excited to an energy corresponding to the $D^*(n=2)$ excited state, the Morse potential is slowly switched off leaving all the Coulomb interactions between the five particles. This latter change is made so that the $D^+ + D^*(n=2)$ interaction replicates the true molecular potentials that are basically molecular Rydbergs of D_2^{2+} for internuclear separations less than 5 a.u.

In our theoretical model the energy required to remove both electrons from D_2 is the sum of the ionization energies for the two electrons (27.2 eV), the dissociation energy of D_2 to its separated atoms (4.7 eV), and the approximately 19 eV required to place the two protons on the repulsive Coulomb potential at a D_2 equilibrium separation of 1.40 a.u. Our model reproduces the experimental energy of 51 eV required to remove both electrons in a vertical Franck-Condon transition. Loss of flux due to single-electron removal is inherently included in the model. Moreover, if the molecular bond length of the D_2 or D_2^+ state is changed during the collision, the corresponding energy required for double-electron removal will differ from that of a vertical Franck-Condon transition. These bond length changes may be induced by the additional presence of the highly charged ion in slow collisions, where the dissociation time is comparable to that of the collision.

In Fig. 9 we show the results of the CTMC calculations of the slices shown in Fig. 8. All conditions and views are the same as in Fig. 8, except that calculations for 382-eV/u Xe have not been performed. The agreement with the experimental results is remarkable, and confirms both the ability of the CTMC formulation to account for the physical processes occurring and our interpretation of the effects observed.

IV. CONCLUSIONS

In conclusion, using three-dimensional momentum imaging techniques we have performed a kinematically complete measurement of the dissociation of D_2 in collision with slow Xe^{26+}. The momentum transferred from the projectile to the center of mass of the molecule (**K**) was separated from the relative momentum of the deuterons measured in the center-of-mass system of the molecule **k**. The latter is dominated by

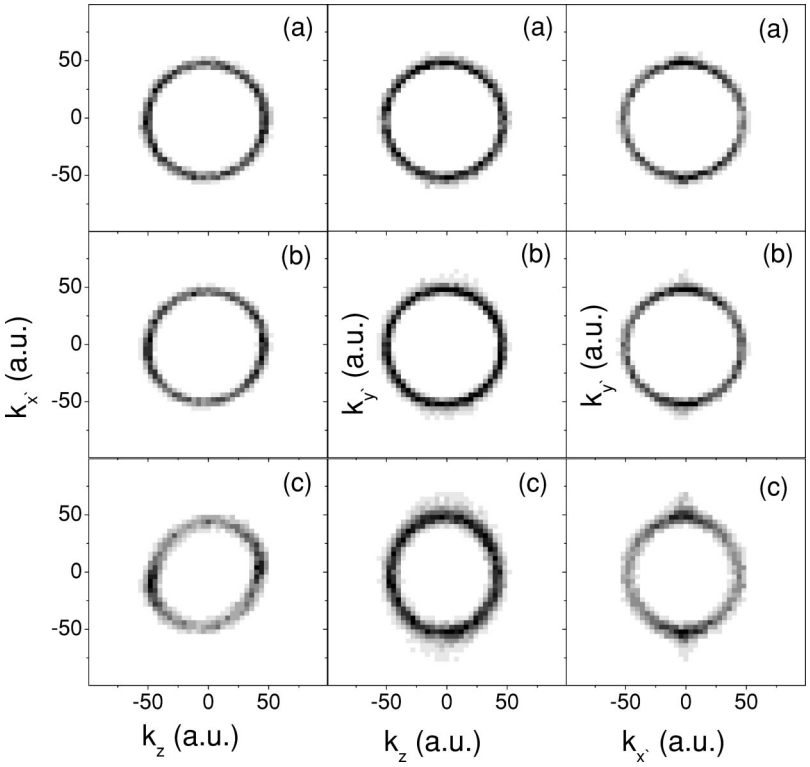

FIG. 9. CTMC calculations of momentum slices corresponding to Fig. 8. The collision systems, proceeding from top to bottom, are for Xe^{26+} energies of 9.56 keV/u, 764 eV/u, and 191 eV/u.

momentum gained through the Coulomb repulsion of the ions pairs emitted in the dissociation of D_2. The overall dissociation mechanism was observed to be dominated by a two-step process, in which these two momentum-transfer processes can be considered to occur as independent events. The **K** distributions were found to be in agreement with expectations based on the extended classical overbarrier model, and established systematics for double capture by slow, highly charged projectiles. At the lowest projectile velocities, the two-step picture was found to fail. The **k** spectra show that internal energy is extracted from the molecular system by the projectile. This was attributed to the presence of the projectile during the dissociation process. A qualitative model was suggested for the interpretation of our results, involving the action of quadrupole (and higher) components of the projectile field on the exploding molecule. CTMC calculations were performed and found to be in excellent agreement with the experimental data. We note that different systematics are likely to apply for capture reactions for which smaller impact parameters are involved, and the projectile passes inside the physical extent of the molecule. Investigations of such systems would be of great interest in this regard.

ACKNOWLEDGMENTS

This work was supported by the Division of Chemical Sciences, Office of Basic Energy Sciences, Office of Energy Research, and the U.S. Department of Energy.

[1] G. Dugardin, S. Lenach, O. Dutuit, P.-M. Gyon, and M. Richard-Viard, Chem. Phys. **88**, 339 (1984).
[2] F.B. Yousif, B.G. Lindsay, and C.J. Latimer, J. Phys. B **23**, 495-504 (1990).
[3] A.K. Edwards, R.M. Wood, and M.F. Steuer, Phys. Rev. A **15**, 48 (1977).
[4] R.M. Wood, A.K. Edwards, and M.F. Steuer, Phys. Rev. A **15**, 1433 (1977).
[5] A.K. Edwards and R.M. Wood, J. Chem. Phys. **23**, 1491 (1990).
[6] B. Brehn and G. de Frenes, Int. J. Mass Spectrom. Ion Phys. **26**, 251 (1978).
[7] I. Ali, R. Dörner, O. Jagutzki, S. Nüttgens, V. Mergel, L. Spielberger, Kh. Khayyat, T. Vogt, H. Bräuning, K. Ullmann, R. Moshammer, J. Ullrich, S. Hagmann, K.-O. Groenefeld, C.L. Cocke, and H. Schmidt-Böcking, Nucl. Instrum. Methods Phys. Res. B **149**, 490 (1999).
[8] R. Dörner, J. Ullrich, R.E. Olson, O. Jagutzki, and H. Schmidt-Böcking, Phys. Rev. A **47**, 3845 (1993).
[9] R. Ali, C.L. Cocke, M.L. Raphaelian, and M. Stöckli, J. Phys. B **26**, L177 (1993).
[10] L. Spielberger, O. Jagutzki, R. Dörner, J. Ullrich, U. Meyer, M. Unverzagt, M. Damrau, T. Vogt, I. Ali, Kh. Khayyat, D. Bahr, H.G. Schmidt, R. Frahm, and H. Schmidt-Böcking, Phys. Rev. Lett. **74**, 4615 (1995).
[11] J. Ullrich, R. Moshammer, R. Dörner, V. Mergel, O. Jagutzki, H. Schmidt-Böcking, and L. Spielberger, J. Phys. B **30**, 2917 (1997).

[12] V. Mergel, R. Dörner, J. Ulrich, O. Jagutzki, S. Lencinas, S. Nttgens, L. Spielberger, M. Unverzagt, C.L. Cocke, R.E. Olson, M. Schulz, U. Buck, and H. Schmidt-Böcking, Nucl. Instrum. Methods Phys. Res. B **98**, 593 (1995).
[13] A.G. Suits and R.E. Continetti, *Imaging in Chemical Dynamics*, A.C.S. Symposium Series Vol. 770 (American Chemical Society, Washington DC, 2000), p. 1.
[14] C.J. Wood, and R.E. Olson, Phys. Rev. A **59**, 1317 (1998).
[15] C.R. Feeler, R.E. Olson, R.D. DuBois, T. Schlathölter, O. Hadjar, R. Hoekstra, and R. Morgenstern, Phys. Rev. A **60**, 2112 (1999).
[16] V.V. Afrosimov, G.A. Leiko, and M.N. Panov, Sov. Phys. Tech. Phys. **25**, 313 (1980).
[17] J.P. Giese *et al.*, Phys. Rev. A **38**, 4494 (1988).
[18] R.D. DuBois *et al.*, Europhys. Lett. **49**, 41 (2000).
[19] F. Freemont, C. Bedouet, M. Tarisien, L. Adoui, J.-Y. Chesnel, and X. Husson, J. Phys. B **33**, L249-L258 (2000).
[20] H.O. Folkerts, R. Hoekstra, and R. Morgenstern, Phys. Rev. Lett. **77**, 3339 (1996).
[21] R.D. DuBois, I. Ali, C.L. Cocke, C.R. Feeler, and R.E. Olson, Phys. Rev. A **62**, 060701(R) (2000).
[22] M. Barat and P. Roncin, J. Phys. B **25**, 220 (1992).
[23] E.K. Janev and H. Winter, Phys. Rep. **117**, 265 (1985).
[24] A. Niehaus, J. Phys. B **19**, 2925 (1986).
[25] M.A. Abdallah, W. Wolff, H.E. Wolf, C.L. Cocke, and M. Stöckli, Phys. Rev. A **58**, 3379 (1998).
[26] R. Ali, V. Frohne, C.L. Cocke, M. Stöckli, and M.L.A. Raphaelian, Phys. Rev. Lett. **69**, 2491 (1992).
[27] C.J. Wood and R.E. Olson, Phys. Rev. A **59**, 1317 (1999).
[28] G. Herzberg, *Spectra of Diatomic Molecules* (Van Nostrand, Princeton, 1950), p. 532.